DOI: 10.13009/EUCASS2017-353

A hybrid LST-RANS method for modelling of laminar-turbulent transition

Alexander Fedorov and Anton Obraz***
**Central Aerohydrodynamic Institute*
Zhukovsky str., 1, Zhukovsky, Russia
***Moscow Institute of Physics and Technology*
Zhukovsky str., 18, Zhukovsky, Russia

Abstract

A new boundary layer intermittency model based on linear stability theory and e-N method is presented. The intermittency depends on the turbulent spot formation rate function. Unlike other models the spot formation rate is not treated empirically but obtained from characteristics of unstable wave packets causing laminar-turbulent transition. These characteristics as well as the transition onset are determined using the linear stability theory and the e-N method. The proposed intermittency model is incorporated into the Spalart-Allmaras RANS model. Numerical simulations of laminar, transitional and turbulent flow are made for two-dimensional configurations (flat plate and circular cone at zero angle of attack) in a wide range of free-stream parameters (Mach number from 0.04 to 7.93 and wall temperature factors from 0.07 to 1). For all cases considered, transition is due to amplification of Tollmien-Schlichting waves for subsonic flows or the Mack second mode for hypersonic flows. Predicted distributions of the heat-flux and viscous-drag coefficients are compared with experimental data.

Introduction

The flight quality of aircrafts and aerospace systems highly depends on the state of boundary-layer flow. Characteristics of laminar and turbulent boundary layers, such as drag coefficient, heat flux coefficient, extent of separation zones etc. are considerably different. In many practical cases, the following flow regime is observed on the vehicle surface. Near the leading edge the flow is usually laminar. At some point the boundary layer becomes unstable and initially small disturbances grow exponentially downstream. This region is treated in the framework of linear stability theory (LST). Further downstream nonlinear processes destroy the laminar flow and turbulent regime sets in. Thus, there are three characteristic regions: laminar, transitional and turbulent.

Nowadays numerical simulations of such flows are usually carried out using RANS (Reynolds Averaged Navier-Stokes) models. These semi-empirical models, as a rule, are calibrated to predict the well-developed turbulent boundary layer flow. To simulate the transitional flow one should make some modifications of the RANS model. One approach is to add some equations to a particular RANS model, e.g. intermittency transport equation and/or activation of turbulence kinetic energy production/destruction terms in a distributed manner [1]. Although qualitatively resembling the intermittency process, these approaches usually are empirics based and do not take into account the detailed prehistory of the transition to developed turbulence.

For predictions of the transition onset, the state of the art method suitable for practical configurations and engineering studies is the e-N method [2],[3], which is based on the linear stability theory (LST). There are numerous attempts to couple a RANS solver with an e-N LST solver and develop a hybrid RANS-LST code (see, for example, [4],[5]). While predicting the transition onset in a physics-based manner, this approach does not simulate the transitional region associated with the nonlinear breakdown. To remedy this defect, empirical correlations for the intermittency are usually integrated into the RANS model, e.g. [6]. In this case, the transition zone length is a semi-empirical quantity determined using available experimental data.

An attempt to couple LST with RANS in a more physics-based manner was made in [7]. The Reynolds-stresses produced by the most amplified disturbances were evaluated at the transition onset and used as an input for RANS-model. Namely, the Reynolds-stress profiles were derived from the linear stability analysis and the e-N method. Then these profiles were calibrated with the aid of direct numerical simulation data.

DOI: 10.13009/EUCASS2017-353

In this paper, we use the LST analysis to predict not only the transition onset, but also the spot-rate function – a number of turbulent spots originating at a given point per second per unit square of a body surface. This can be done using the physics-based amplitude method developed by Mack [8] and recently applied to hypersonic configurations in [9],[10]. Calculating the spot-rate function and using the spot shape factors available from experiments and DNS data, we compute the intermittency function. The latter is incorporated into the Spalart-Allmaras (SA) turbulence model [11]. Using such a hybrid LST-RANS method, the numerical simulations are conducted for simple geometries (flat plates and circular cones at zero angle of attack). The predicted distributions of heat flux and skin friction are compared with available experimental data.

1. LST analysis

In the framework of linear stability theory for 2D compressible boundary-layer flows [12], the 3D disturbance vector $\mathbf{Q}' = \{u', v', w', p', T'\}^T$ is expressed in the traveling wave form

$$\mathbf{Q}'(x, y, z, t) = \hat{\mathbf{q}}(\omega, \beta; x, y) e^{i(\alpha x + \beta z - \omega t)} \qquad (1.1)$$

where (x, y, z) - Cartesian reference frame with the x - axis directed downstream and y -axis directed normal to the wall, t - time, ω - circular frequency, (α, β) - wavenumber components, (u, v, w) - velocity components, p - pressure and T - temperature. The form (1.1) is valid in the local-parallel approximation. The shape-function $\hat{\mathbf{q}}(y; x)$ is a solution of the local eigenvalue problem consisting of the linear stability equations and homogeneous boundary conditions on the wall ($\hat{q}_{1,2,3,5}(0) = 0$) and outside the boundary layer ($\hat{q}_{1,2,3,5}(\infty) = 0$). Assuming that β and ω are real quantities, the complex eigenvalue $\alpha(\omega, \beta; x) = \alpha_r + i\alpha_i$ corresponds to one of the boundary-layer modes of the discrete spectrum. For 2D flows considered herein, these could be Tollmien-Schlichting (TS) waves (at subsonic speeds), the first and/or second mode (at supersonic and hypersonic speeds). The local growth rate is determined as $\sigma = -\alpha_i(\omega, \beta; x)$.

Following Mack [8] we assume that in natural transition phase shifts between waves of a particular mode are random so that the wave amplitudes add in the square. In this case the average square of a certain physical quantity $q(x, y, t)$ related to the disturbance is written as:

$$\left\langle q^2 \right\rangle(x, y) = \int_{-\infty}^{\infty} d\omega \int_{-\infty}^{\infty} A_0^2(\omega, \beta; x_0) \left| \hat{q}(\omega, \beta; x, y) \right|^2 e^{2N(\omega, \beta; x)} d\beta \qquad (1.2)$$

$$N(\omega, \beta; x) = \int_{x_0}^{x} \sigma dx \qquad (1.3)$$

where N is the integral amplification or N-factor, $x_0(\omega, \beta)$ is the neutral point of a particular wave; $A_0(\omega, \beta; x_0)$ is the wave amplitude at the neutral point, which is treated as an initial amplitude, $\left\langle \ \right\rangle$ denotes ensemble averaging.

It is assumed that the initial amplitudes weakly depend on ω and β (the initial spectrum is broad). Then the power spectral density of the random disturbance q can be approximated by the Gaussian function. Namely, in the observation station x the N-factor has maximum at ω_c and β_c determined by the conditions

$$\partial_\beta N(\omega_c, \beta_c; x) = 0, \ \ \partial_\omega N(\omega_c, \beta_c; x) = 0 \qquad (1.4)$$

In the vicinity of (ω_c, β_c) the N-factor is expanded as:

$$2N(\omega, \beta; x) = 2N(\omega_c, \beta_c; x) + \partial^2_{\omega\omega} N(\omega_c, \beta_c; x)(\omega - \omega_c)^2 + \partial^2_{\beta\beta} N(\omega_c, \beta_c; x)(\beta - \beta_c)^2 + \ldots \qquad (1.5)$$

where the mixed derivative $N_{\omega\beta}$ is omitted because we consider instabilities having $\beta_c = 0$ for all frequencies; i.e. the most unstable are plane waves and $\partial / \partial\beta$ is zero.

With the help of (1.2) and (1.5) the power spectral density is expressed as

DOI: 10.13009/EUCASS2017-353

$$S(\omega,\beta;y,x) \approx \frac{1}{2\pi} S_c(x,y) \exp\left[-\frac{(\omega-\omega_c)^2}{2\sigma_\omega^2} - \frac{(\beta-\beta_c)^2}{2\sigma_\beta^2}\right], \qquad (1.6a)$$

$$\sigma_\omega^2 = -\frac{1}{2\partial^2_{\omega\omega} N(\omega_c,\beta_c;x)},\ \sigma_\beta^2 = -\frac{1}{2\partial^2_{\beta\beta} N(\omega_c,\beta_c;x)} \qquad (1.6b)$$

The correlation function $R_q(\tau,\zeta) \equiv \left\langle q(t,z)q(t+\tau,z+\zeta)\right\rangle$ is calculated as:

$$R_q(\tau,\zeta) = \frac{1}{2\pi}\int_{-\infty}^{+\infty} S(\omega,\beta) e^{i\omega\tau + i\beta\zeta} d\omega d\beta$$

Available experimental data show that in transitional boundary layers turbulent spots originate when fluctuating quantities exceed certain threshold values. For example, in the case of hypersonic boundary layers over a flat plate, where transition is dominated by the Mack second mode, turbulent spots emerge when the RMS level of u'-fluctuations exceeds approximately 5% of the boundary-layer edge velocity. In order to predict the spot-rate function it is important to calculate the average frequency ν_t of exceeding the threshold level a. This can be done using the theory of random processes [13], which gives the relations

$$\nu_t = \frac{\sigma_v}{2\pi\sigma} e^{-\frac{a^2}{2\sigma^2}}$$

$$\sigma^2 = R_u(0), \sigma_v^2 = -\frac{d^2 R_u}{d\tau^2}(0),$$

$$R_u(\tau) = \left\langle u'(t)u'(t+\tau)\right\rangle,$$

where $\sigma^2 = 2S_c = u_{RMS}^2$, $\sigma_v^2 = u_{RMS}^2\sigma_\omega^2$, and u_{RMS} is root-mean-square of u'-fluctuations at the observation point. A similar approach can be applied to calculate the average spatial frequency ν_z of exceeding the threshold level a of u'-fluctuations versus the lateral coordinate z.

With the assumption that a turbulent spot originates every time $u_{RMS} > a$, the average number of turbulent spots generated in the intervals $\left[z, z+\Delta z\right]$ and $\left[t, t+\Delta t\right]$ is calculated as:

$$dN = \nu_t \nu_z dt dz = \frac{\sigma_\omega(x,z)\sigma_\beta(x,z)}{4\pi^2} e^{-\frac{a^2}{u_{RMS}^2(x,z)}} dt dz \qquad (1.7)$$

For 2D mean flows the dispersions $\sigma_\omega, \sigma_\beta$ do not depend on time and z-coordinate, and a turbulent spot formation rate function is expressed in the simple analytical form:

$$g(x) = \frac{dN}{dz dt} = \frac{\sigma_\omega(x)\sigma_\beta(x)}{4\pi^2} e^{-\frac{a^2}{u_{RMS}^2(x)}} \qquad (1.8)$$

2. Intermittency model

Using the model developed by Narasimha [14], the intermittency for 2D boundary-layer flows is expressed as

$$\gamma = 1 - \exp\left\{-\frac{\sigma}{U_e} \mathrm{g}(x_{tr})(x-x_{tr})^2\right\} \qquad (2.1)$$

DOI: 10.13009/EUCASS2017-353

where g_n is the turbulent spot formation rate function, σ is the turbulent spot shape factor and U_e is flow speed at the upper boundary-layer edge, x_{tr} is the transition onset location coordinate.

The function g can be calculated using (1.8). Assuming that at the onset of transition exponential multiplier $\exp(-a^2 / u^2_{RMS}(x_{tr}))$ is nearly a constant value A, we obtain

$$g(x_{tr}) = A\sigma_\omega(x_{tr})\sigma_\beta(x_{tr}) \qquad (2.2)$$

and express the intermittency in the form suitable for practical applications:

$$\gamma = 1 - \exp\left\{-\frac{(x - x_{tr})^2}{\lambda^2}\right\}, \quad \lambda = \left(\frac{U_e}{\sigma A \sigma_\omega \sigma_\beta}\right)^{1/2} \qquad (2.3)$$

Here λ characterizes the transition length. For a flat plate boundary layer the transition length is usually defined as $\lambda_N = x\Big|_{\gamma=0.75} - x\Big|_{\gamma=0.25}$, and the relation (2.1) is written in the form

$$\gamma = 1 - \exp\left[-0.41\frac{(x - x_{tr})^2}{\lambda_N^{\,2}}\right], \ \lambda_N = \lambda / 1.56 \qquad (2.4)$$

Chen & Thyson [15] modified the relationship (2.3) for axisymmetric flows as:

$$\gamma = 1 - \exp\left[-g x_{tr}\frac{x - x_{tr}}{U_e}\ln\frac{x}{x_{tr}}\right] \qquad (2.5)$$

Comparing (2.5) to (2.4) we obtain the formula convenient for numerical implementation:

$$\gamma = 1 - \exp\left[-0.41\frac{x - x_{tr}}{\lambda_N}\frac{x_{tr}}{\lambda_N}\ln\frac{x}{x_{tr}}\right] \qquad (2.6)$$

According (2.3) the transition length λ essentially depends on the shape factor σ. Assuming that the shape of turbulent spots can be approximated by triangle, the shape factor is expressed as [16]:

$$\sigma = \frac{\overline{c}_f - \overline{c}_r}{\overline{c}_r\overline{c}_f}\,\mathrm{tg}\alpha \qquad (2.7)$$

Here $\overline{c}_f = c_f / U_e$ ($\overline{c}_r = c_r / U_e$) is a speed of the spot leading (rear) edge, and α is half-angle of the spot lateral spreading. For example, in the incompressible boundary layer on a flat plate $\overline{c}_f \approx 0.9$, $\overline{c}_r \approx 0.4$, $\alpha \approx 10^\circ$ and $\sigma \approx 0.25$ [14]. Experiments show [17],[18] that $(\overline{c}_f - \overline{c}_r)/(\overline{c}_r\overline{c}_f)$ and α strongly depends on the local Mach number M_e and the wall temperature ratio T_w / T_e. Herein the distributions of α and $(\overline{c}_f - \overline{c}_r)/(\overline{c}_r\overline{c}_f)$ versus M_e were obtained using the data of Fisher [19] (red line in Fig.1). The dependence on T_w / T_e is not taken into account because of shortage of available data.

Note that in the model of Narasimha [14] both the transition onset point x_{tr} and the transition length λ_N are determined empirically. In our LST-RANS model the transition length is calculated using dispersion characteristics of unstable wave packets at the transition onset x_{tr} (see Eq. (2.3)). The latter can be evaluated with the help of the e^N method by solving the equation

$$\max_{\omega,\beta}\left[N(\omega,\beta;x_{tr})\right] = N_{tr}$$

where N_{tr} is determined empirically.

The expression (2.3) for the transition length λ contains the constant A, which can be evaluated once and for all using a reliable set of experimental data. Consider the transition experiment [20] on a flat plate in the Low-Mach wind tunnel ($M_e \approx 0.04$), where the intermittency $\gamma(x)$ was measured at various unit Reynolds numbers. The LST

DOI: 10.13009/EUCASS2017-353

computations are performed for TS waves in the case of $\mathrm{Re}_{tr} \equiv x_{tr} U_e / \nu_e = 2.31 \times 10^6$. Since TS waves are most unstable at $\beta = 0$ for all frequencies, N-factors are computed for plane waves only. The dispersion characteristics of TS wave-packets at the transition onset point x_{tr} are performed as follows:1) Equations (1.4) are solved to determine the wave-packet central frequency ω_c; 2) the second derivatives $\partial^2_{\omega\omega} N(\omega_c, 0; x_{tr})$ and $\partial^2_{\beta\beta} N(\omega_c, 0; x_{tr})$ are computed to evaluate the dispersions σ_ω and σ_β from (1.6b); 3) the length λ is computed using (2.3) with the form factor $\sigma = 0.25$; 4) the intermittency $\gamma(x)$ is computed using (2.3) and compared with the experiment. Steps 3) and 4) were performed at various values of the constant A, and it was found that $A = 0.072$ provided the best fit to the experimental distribution of $\gamma(x)$ as shown in Fig. 2.

Further computations were carried out for transitional boundary layers at supersonic and hypersonic speeds, where characteristics of turbulent spots were orders of magnitude different from the foregoing subsonic case. Nevertheless, in all cases considered hereafter, the constant A was fixed and equal 0.072.

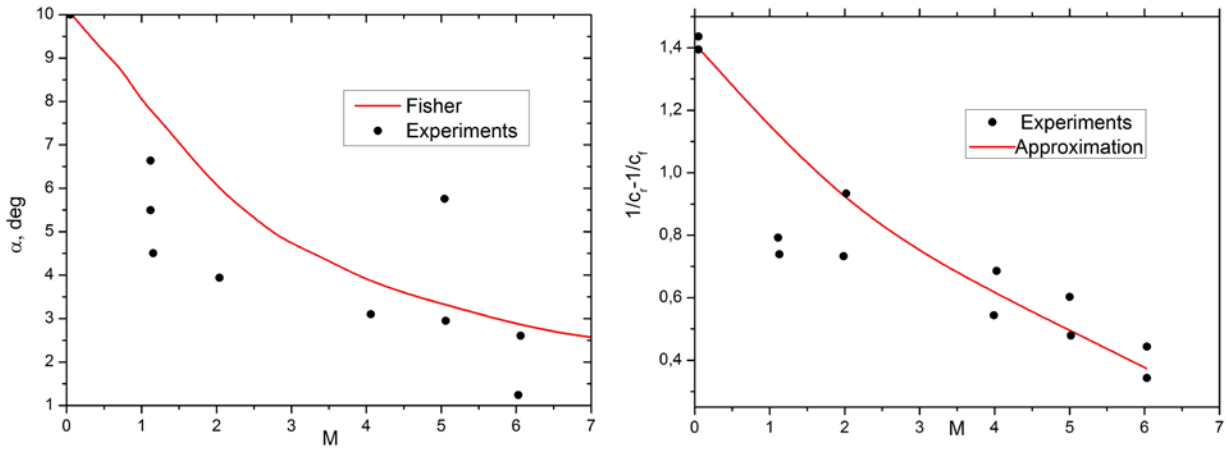

Fig.1
Approximations of the spreading angle of a turbulent spot and phase factor versus Mach number used in this work (dots are available experimental data from [17],[18],[19]).

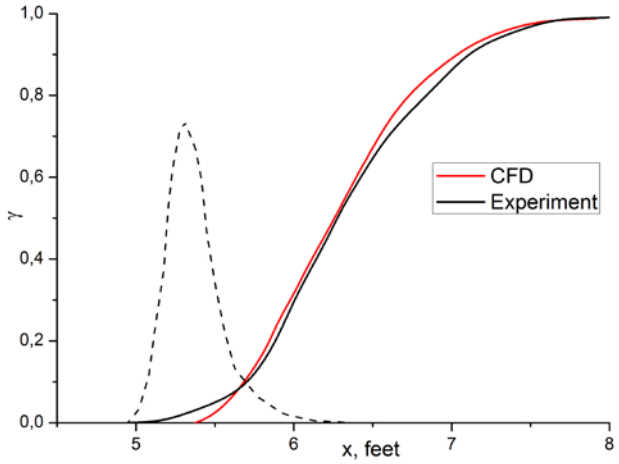

Fig.2
Comparison between experimental measurements of intermittency [20] (black line) and calculations with our model (red line). Dotted line is the schematic spot-rate function distribution.

DOI: 10.13009/EUCASS2017-353

3. RANS model & CFD code

TsAGI's in-house CFD solver HSFlow [21] was used to make all RANS-based numerical calculations in this paper. It is a finite volume method which solves full Navier-Stokes equations in the conservative form

$$\frac{\partial \mathbf{Q}}{\partial t}+\frac{\partial \mathbf{E}}{\partial x}+\frac{\partial \mathbf{G}}{\partial y}+\frac{\partial \mathbf{F}}{\partial z}=\mathbf{0} \qquad (3.1)$$

directly (DNS) or with various RANS closures. Here $\mathbf{Q}$ is the conservative vector of unknowns and $\mathbf{E},\mathbf{F},\mathbf{G}$ are flux vectors. Herein the SA turbulence model is used, where:

$$\mathbf{Q}=\{\rho,\rho u,\rho v,\rho e,\rho\overline{\nu}_t\}^T \qquad (3.2)$$

Here ν_t is the eddy viscosity calculated via $\overline{\nu}_t$ with the wall function $f_{\nu 1}$: $\nu_t=\overline{\nu}_t f_{\nu 1}$, and the equation for the value $\overline{\nu}_t$ is

$$\frac{\partial(\rho\overline{\nu}_t)}{\partial t}+\frac{\partial}{\partial x_j}(\rho\overline{\nu}_t u_j)=C_{B1}\rho S\overline{\nu}_t+\frac{1}{\sigma}[\frac{\partial}{\partial x_j}(\rho(\nu+\overline{\nu}_t)\frac{\partial\overline{\nu}_t}{\partial x_j})+C_{B2}\rho\frac{\partial\overline{\nu}_t}{\partial x_j}\frac{\partial\overline{\nu}_t}{\partial x_j}]-C_{w1}f_w\rho(\frac{\overline{\nu}_t}{d})^2 \qquad (3.3)$$

Here all trip terms that internally control the transitional behavior of the model are disabled. Expressions for basic parameters of the SA model can be found in [22]. We use the standard version of the model with the only modification – the eddy viscosity is controlled using the intermittency factor as:

$$\nu=\nu_{lam}+\gamma\nu_t \qquad (3.4)$$

where ν_{lam} is for molecular viscosity. Note that the production and destruction terms in (3.3) are not modified that may unbalance the model. This issue will be clarified in our further studies.

4. Computational results

For all cases considered herein the first-order in time and second-order in space TVD scheme was used. The converged stationary solution with the modified SA model was obtained in 2D plane or axisymmetric computational domains.

4.1 Flat plate experiment, M_e=4.95

The boundary-layer flow on a flat plate is considered at the free-stream Mach number $M_\infty=5$. The flow parameters correspond to the experiment [23] in the shock tunnel UT1M (TsAGI). The Reynolds number based on the free-stream parameters and the model length is $\mathrm{Re}=5.6\times10^7$. The temperature factor (the ratio of the wall temperature to the stagnation temperature) is $T_w/T_0=0.55$. It is assumed that transition is dominated by the second mode. The critical N-factor for the facility is evaluated as $N_{tr}=4.5$. The heat flux to the model surface was measured with temperature sensitive paint and presented as distributions of Stanton number St on the model surface.
The LST-RANS computations were carried out on the computational grid with 200 nodes in the streamwise direction and 220 nodes in the wall normal direction. More than 15 nodes were in the laminar sub-layer of the turbulent flow part at the onset of transition. Approximately 120 nodes were inside the boundary layer near the outflow boundary of the computational domain. For the all the cases considered, similar grids were used.
The predicted distribution of $St(x)$ is compared with the experiment in Fig.3. A satisfactory agreement for the transition length is obtained. The predicted heat fluxes are 10% -15% higher than in the experiment.

DOI: 10.13009/EUCASS2017-353

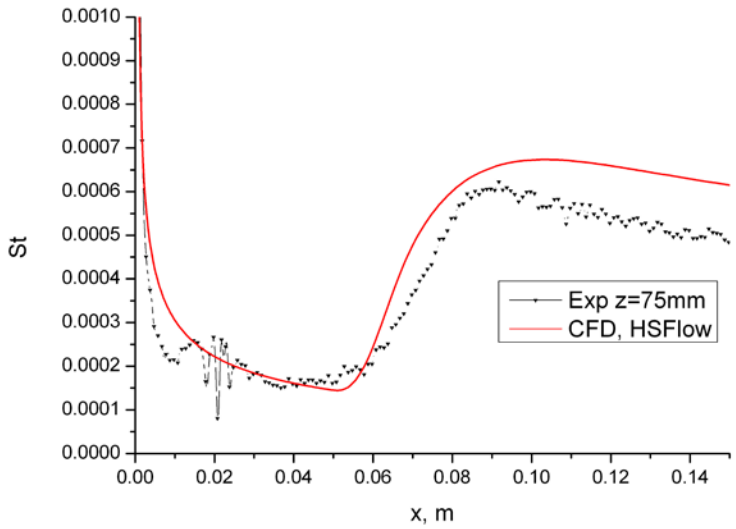

Fig.3
Comparison of wall heat flux distributions for a flat plate from Section 4.1. Black dots – experimental data [23], red line – CFD calculation with our model.

4.2 Sharp cone at zero AoA, M_e=5.3

A flow past a 7 degree half-angle sharp circular cone at $M_\infty = 6$ is considered. The flow parameters corresponds to the experiment [24] in the VKI H3 wind tunnel (von Karman Institute). The Mach number at the upper boundary-layer edge is M_e=5.3 at the transition onset point. The Reynolds number based on the free-stream parameters and the cone length is $\mathrm{Re} = 2.2 \times 10^7$, the temperature factor is $T_w / T_0 = 0.53$. It is assumed that transition is dominated by the second mode. At the transition onset point $x_{tr} = 144\,mm$ the critical N-factor is $N_{tr} = 5.3$.

Figure 4 compares the heat-flux distributions. Both laminar and turbulent levels of St are predicted satisfactory by the LST-RANS model, while the transition length is slightly greater than in the experiment. The modified SA model does not give an overshoot near the transition end, which is observed experimentally.

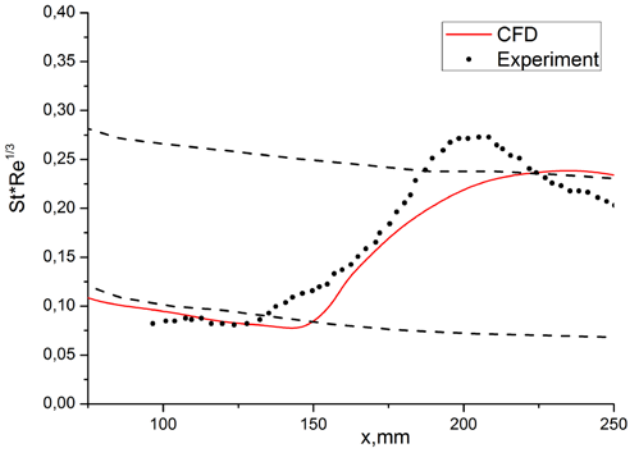

Fig.4
Comparison of wall heat flux distributions for a sharp cone from Section 4.2. Black dots – experimental data [24], red line – CFD calculation with our model.

4.3 Sharp circular cone, M_e=5.5

DOI: 10.13009/EUCASS2017-353

A flow past a 5 degree half-angle sharp circular cone at $M_\infty = 6$. The flow parameters correspond to the experiment [25] conducted in the high-enthalpy shock tunnel T5 (CalTech). The local Mach number at the transition onset point is M_e=5.5. The Reynolds number based on the free-stream parameters and the cone length is $\mathrm{Re} = 5.56 \times 10^6$, and the wall temperature factor is about 0.07. It is assumed that transition is dominated by the second mode. At the transition onset point the critical N-factor is $N_{tr} = 6.6$.

The longitudinal distributions of the heat flux were measured by calorimeters and presented as $St(\mathrm{Re}_x)$, where $\mathrm{Re}_x = \nu_\infty U_\infty x$. As shown in Fig. 5, the predicted distributions $St(\mathrm{Re}_x)$ agree very well with the experiment in laminar, transitional and turbulent regions.

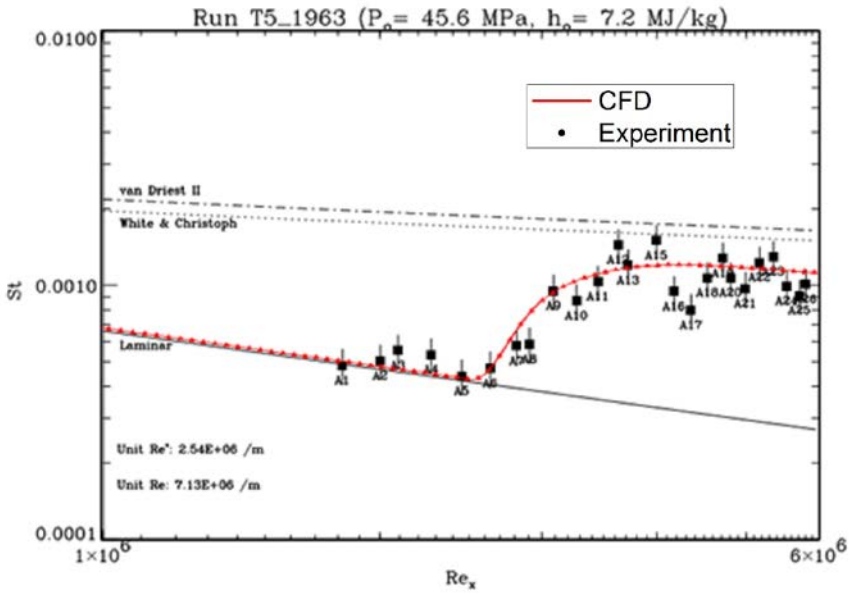

Fig.5

Comparison of wall heat flux distributions for a sharp cone from Section 4.3. Black dots – experimental data [25], red line – CFD calculation with our model.

4.4 Flat plate at M_e=5.95

A flow past a flat plate at $M_\infty = 6$ is considered. The flow parameters correspond to the experiment [26] conducted in the NASA Langley M6 wind tunnel. The CFD studies of this experiment are discussed in [27]. The Reynolds number based on the free-stream parameters and the model length is $\mathrm{Re} = 2.64 \times 10^7$, the temperature factor is $T_w / T_0 = 0.6$. It is assumed that transition is dominated by the second mode. At the transition onset point the critical N-factor is $N_{tr} = 5.3$. The heat flux distribution was measured along the plate surface. As shown in Fig. 6, the predicted distribution of $St(\mathrm{Re}_x)$ and the transition length agree well with the experiment.

DOI: 10.13009/EUCASS2017-353

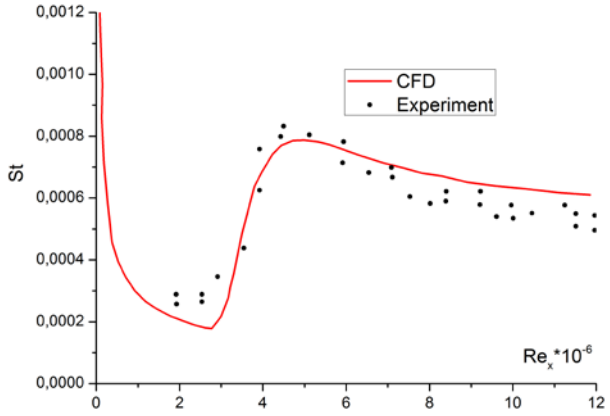

Fig.6
Comparison of wall heat flux distributions for a flat plate from Section 4.4. Black dots – experimental data [26], red line – CFD calculation with our model.

4.5 Sharp cone at M_e=6.82

A flow past a 7-degree half-angle sharp cone is considered at $M_\infty = 7.93$ and zero angle of atack. The flow parameters correspond to the experiment [28] conducted in the AEDC tunnel B (Arnold Engineering Development Center). The Reynolds number based on the free-stream parameters on the cone length L is $\mathrm{Re} = 6.6 \times 10^6$, the temperature factor is $T_w / T_0 = 0.39$. It is assumed that transition is dominated by the second mode. At the transition onset point $x_{tr} = 0.36$ the critical N factor is $N_{tr} = 5.4$. The heat flux distribution is measured along the cone surface and presented as $Ch(\overline{x})$, $\overline{x} = x / L$. AS shown in Fig. 8, the LST-RANS prediction agrees satisfactorily with the experiment.

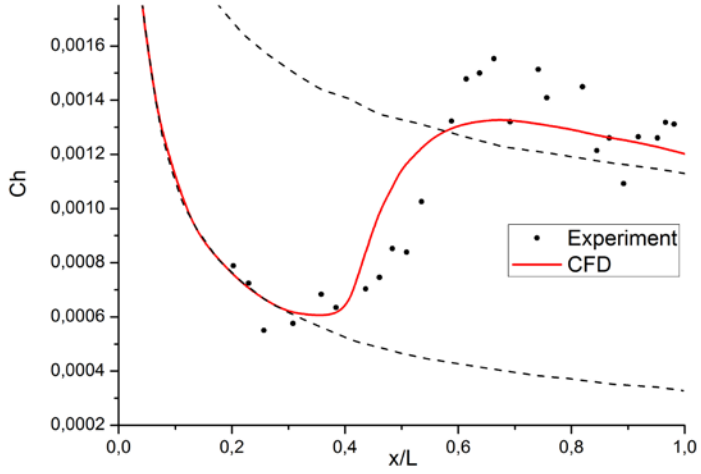

Fig.7
Comparison of wall heat flux distributions for a flat plate from Section 4.5. Black dots – experimental data [28], red line – CFD calculation with our model.

5. Conclusions

A new physics-based LST-RANS model is developed for holistic modelling of transitional boundary layers. Namely, the linear stability theory is used to predict the transition onset with the help of e^N method and dispersions of

DOI: 10.13009/EUCASS2017-353

unstable wave-packets at the transition onset point are computed. The latter are used to evaluate the turbulent spot formation rate function and predict the intermittency function. The new intermittency model contains only one empirical constant, which was determined using the experimental data obtained on a flat plate model in the low-Mach wind tunnel. The intermittency calculation method was incorporated in the turbulence model of Spallart and Allmaras.

The hybrid LST-RANS model is validated using available experimental data for 2D and axisymmetric boundary-layer flows on flat plates and sharp cones at zero angle of attack tested in different supersonic and hypersonic wind tunnels. For the all cases considered, it was assumed that transition is dominated by the second mode. In the ranges of the free-stream Mach number from 5 to 8 and the temperature factor T_w / T_0 from 0.07 to 0.6, the heat-flux distributions, predicted in laminar, transitional and turbulent regions, agree satisfactorily with the experiment.

These findings encourage us to continue the study. It is planned to extend the proposed LST-RANS model to the cases where transition is dominated by oblique waves such as the first mode and cross-flow instability. It is also important to treat 3D boundary-layer flows relevant to realistic supersonic and hypersonic configurations.

Acknowledgement

The work was supported by Russian Scientific Foundation (Project №14-19-00821).

References

1. F. R. Menter, R. Langtry, and S. Völker, “Transition modelling for general purpose CFD codes,” *Flow Turbul. Combust.*, vol. 77, pp. 277–303, 2006.
2. J. L. V. Ingen, “A Suggested Semi-empirical Method for the Calculation of the Boundary Layer Region,” TU Delft, VTH17, 1956.
3. A.M.O. Smith, N. Gamberoni, “Transition, Pressure Gradient and Stability Theory,” Douglas Aircraft Company, ES 26388, 1956.
4. A. Krumbein, “Application of a Hybrid Navier-Stokes Solver with Automatic Transition Prediction,” *AIAA Paper*, 2007.
5. S. Fu and L. Wang, “RANS modeling of high-speed aerodynamic flow transition with consideration of stability theory,” *Progress in Aerospace Sciences*, vol. 58, pp. 36–59, 2013.
6. S. McKeel, “Numerical simulation of the transition region in hypersonic flow”, PhD Thesis, Virginia polytechnic institute, 1996.
7. A. Probst, R. Radespiel, and U.Rist, “Linear-Stability-Based Transition Modeling for Aerodynamic Flow Simulations with a Near-Wall Reynolds-Stress Model,” *AIAA J.*, vol. 50, no. 2, pp. 416–428, 2012.
8. L. M. Mack, “Transition and Laminar Instability,” Jet Propulsion Lab, Pasadena, Calif., NASA-CP-153203, May 1977.
9. A. V. Fedorov, “Receptivity of a supersonic boundary layer to solid particulates,” *J. Fluid Mech.*, vol. 737, pp. 105–131, 2013.
10. A.V. Fedorov, “Receptivity of High-Speed Boundary Layers to Kinetic Fluctuations,” *AIAA J.*, Article in Advance, DOI: 10.2514/1.J055326, 2017.
11. P. R. Spalart and S. R. Allmaras, “A One-Equation TurbulenceModel for Aerodynamic Flows,” *La Recherche Aérospatiale*, vol. Vol. 1, pp. 5–21, 1994.
12. W. O. Criminale, T. L. Jackson, and R. D. Joslin, *Theory and Computation of Hydrodynamic Stability*. Cambridge: Cambridge University Press, 2003.
13. A. M. Yaglom, *Correlation Theory of Stationary and Related Random Functions: Supplementary Notes and References*. Springer New York, 2012.
14. R. Narasimha and S. Dhawan, “Some Properties of Boundary Layer Flow During the Transition from Laminar to Turbulent Motion,” *Journal of Fluid Mechanics*, vol. 3, pp. 418–436, 1958.
15. K. Chen and A. Thyson, “Extension of Emmons Spot Theory for Blunt Bodies,” *AIAA Journal*, vol. 9, no. 5, pp. 821–825, 1971.
16. H. W. Emmons, “The Laminar-Turbulent Transition in a Boundary Layer —Part I,” *J. Aero. Sci.*, vol. V.18, no. 7, pp. 490–498, 1951.

DOI: 10.13009/EUCASS2017-353

17. A. Jocksch, “Growth of turbulent spots in high-speed boundary layers,” *International J. of Heat and Fluid Flow*, vol. 29, no. 6, pp. 1543–1557, Dec. 2008.
18. L. Krishnan and N. D. Sandham, “Effect of Mach number on the structure of turbulent spots,” *J. Fluid Mech.*, vol. 566, pp. 225–234, 2006.
19. M. C. Fisher, “Spreading of a Turbulent Disturbance,” *AIAA J.* vol. 10, pp. 957–959, 1972.
20. G. B. Schubauer and P. S. Klebanoff, “Contributions on the Mechanics of Boundary Layer Transition,” NACA-1289, 1955.
21. A. Novikov, I. Egorov, and A. Fedorov, “Direct numerical simulation of wave packets in hypersonic compression corner flow,” *AIAA J.*, vol. 54, no. 7, pp. 2034–2050, 2016.
22. T. J. Coakley, “Turbulence Modeling Validation, Testing and Development,” NASA TP, 1997.
23. A. S. E. Pesetskaya, A. Novikov, “An experimental study of the transitional flow over blunted plate,” TsAGI-10041, 2011.
24. D. Masutti, “Ground Testing Investigation of Hypersonic Transition Phenomena for a Reentry Vehicle,” PhD Thesis, Von Karman Institute for Fluid Mechanics, 2013.
25. A. Rasheed, “Passive Hypervelocity Boundary Layer Control Using an Ultrasonically Absorptive Surface,” PhD Thesis, CalTech, 2001.
26. M. H. Bertram, A. M. Cary, and J. A. H. Whitehead, “Experiments With Hypersonic Turbulent Boundary Layers on Flat Plates and Delta Wings,” AGARD Specialists’ Meeting on Hypersonic Boundary Layers and Flow Fields, 1968.
27. A.D.Dilley, “Evaluation of CFD Turbulent Heating Prediction Techniques and Comparison With Hypersonic Experimental Data,” NASA, CR-2001-210837.
28. R. Kimmel, “The effect of pressure gradients on transition zone length in hypersonic boundary layers,” Wright Lab, WL-TR-94-3012, 1993.